ACADEMIC PRESS

Available online at www.sciencedirect.com

SCIENCE DIRECT®

Journal of Sound and Vibration 270 (2004) 39–59

JOURNAL OF SOUND AND VIBRATION

www.elsevier.com/locate/jsvi

Detection of localised damage in plane circular arches by frequency data

M.N. Cerri[a], G.C. Ruta[b,*]

[a] *Istituto di Scienza e Tecnica delle Costruzioni, Università di Ancona, via Brecce Bianche, 60131 Ancona, Italy*
[b] *Dipartimento di Ingegneria Strutturale e Geotecnica, Università di Roma "La Sapienza", via Eudossiana 18, 00184 Roma, Italy*

Received 9 July 2002; accepted 5 December 2002

Abstract

The possibility to detect the structural damage affecting a narrow zone of a doubly hinged plane circular arch by means of a few measured natural frequencies is considered. Such localised damage induces a discontinuity in the bending stiffness of the arch, modelled as a torsion spring joining two adjacent sections and characterised by the location and the stiffness of the spring. The direct problem in the damaged and undamaged case is examined; the inverse problem is then considered. Two different procedures to identify the damage parameters are introduced: the first is based on the search of an intersection point of curves obtained by the modal equation; the second is based on the comparison between the analytical and experimental values of the variation of frequencies passing from the undamaged to the damaged state. In conclusion, the possibility of identifying the damage parameters by means of pseudo-experimental data is examined.

1. Introduction

In previous years, great attention has been paid in the field of civil engineering to modelling and identifying damage in structures, in particular by means of non-destructive techniques. Some of these techniques detect the damage by measuring dynamical quantities: the structural changes induced by the damage are related with the variations of the dynamical response of the structure. Doebling et al. [1] recently published a review of papers on structural damage detection via vibration data. A mathematical model, either analytical or numerical, of the considered structural

*Corresponding author.
E-mail addresses: cerrimn@mta01.unian.it (M.N. Cerri), giuseppe.ruta@uniroma1.it (G.C. Ruta).

0022-460X/03/$ - see front matter
doi:10.1016/S0022-460X(03)00482-6

element and of the damage is needed; then, the identification of the position and magnitude of the damage may be based on the change: (i) in the natural frequencies; (ii) in the mode shapes; (iii) in the dynamical flexibility of the considered element, and develop into many different techniques [1]. In particular, much study has been devoted to the procedures based on the measurement of natural frequencies in simple elements like beams; a review is given by Salawu [2]. The first to suggest damage detection via measurement of natural frequencies are probably Cawley and Adams [3]. Most of the considered references represent the damage by one or more fully open cracks distributed along the axis of the beam and not altering its mass. This equals to a reduction in the bending stiffness of the beam at the section where the crack is located, or in a restricted portion nearby: damage is supposed to be localised. A beam affected by localised damage may be modelled by two or more different beams hinged with each other and connected by a torsion spring at the damaged sections, as first proposed by Chondras and Dimarogonas [4]. A one-dimensional continuum theory of cracked Euler–Bernoulli beams is due to Christides and Barr [5]. Gladwell [6] focuses on inverse problems for vibrating beams. In the literature on damage detection both numerical and analytical models of beams are present. Yuen [7] simulates a crack simply by reducing the stiffness in an element of a FEM code; other numerical results are provided by Liang et al. [8,9]. Rizos et al. [10] estimate the damage by the change in the mode shapes. Ostachowicz and Krawczuk [11] and Shen and Taylor [12] use equations of motion with boundary conditions satisfying the conditions at the crack. Morassi [13,14] introduces more refined one-dimensional beam models, and another continuum cracked beam theory is provided by Chondras et al. [15]. Narkis [16] introduces a damage identification technique based on the variation of the first two natural frequencies due to the crack. Boltezar et al. [17] provide experimental results on the identification of crack by measurements of natural frequencies of axial and flexural vibrations. Capecchi and Vestroni [18–20] and Cerri and Vestroni [21] introduce the damage detection technique which will be used here. Sinha et al. [22] introduce a simplified form of the crack which can be used in a FEM code.

The dynamics of arches is also well known in the literature on mechanics. The book by Henrych [23] can be considered a comprehensive work both from the theoretical and the numerical point of view, but the treatment of arches and rings as curved beams dates back to the paper by Lamb [24] and the book by Love [25]. A review of the papers on the dynamics of arches may be found in Auciello and De Rosa [26] and in Chidamparam and Leissa [27], where more than 400 references are listed. Because of their geometry, vibrations of arches in the directions normal and tangent to the axis are coupled and depend on many mechanical parameters, such as the shape of the arch cross-section, the span of the arch and its height. Simplified equations for the dynamics of arches may be obtained by neglecting some contributions to the strain and to inertial actions, as studied by Waltking [28] and Den Hartog [29]. Account of centre line extension is taken by Philipson [30]. Other effects, such as rotary and tangential inertia and shear strain, are studied in the papers by Rao and Sundararajan [31], Veletsos et al., who make considerations on the energetic characterisation of vibrations [32], Krishnan et al. [33], Tüfekçi and Arpaci, who propose an original way of solving the equations of motion [34]. A numerical approach to the dynamics of arches is that of Tong et al. [35]. One of the very few papers, to our knowledge, on the natural frequencies of damaged arches is that of Krawczuk and Ostachowicz [36].

The aim of this paper is to extend the studies by Vestroni and Capecchi [18–20] and Cerri and Vestroni [21] to arches, identifying the structural damage affecting a narrow zone of a plane

circular arch using a few measured natural frequencies. An analytical study of the frequency response of a one-dimensional arch model with rigid cross sections is performed at first. Use is made of a continuum model instead of a FEM one because in the simple case considered here analytical expressions are obtained, maybe cumbersome, but easy to manipulate via standard software; therefore, broader conclusions can be drawn.

The arch is assumed to be homogeneous and linearly elastic, and the dimensions of the arch cross-section to be small with respect to the radius of curvature of the axis, so that the shearing strain is negligible. Furthermore, the ratio between the height and the span of the arch is such that the relevant behaviour of the arch is flexural: thus, rotary inertia and axis extension are neglected [25–27]. The second step is to examine the frequency response of the same arch affected by a localised damage, represented either by a notch at a cross-section or by the decrease of the bending stiffness in a narrow zone around the considered section. Hence, the damage is accounted for by introducing a torsion spring joining the two cross sections next to the zone of the localised damage. These two steps provide a full treatment of the direct problem. In the inverse problem the position and the magnitude of the damage must be detected: on this purpose, two procedures are introduced, based on experimental natural frequency measurements in both the undamaged and damaged case. The first procedure is based on the characteristic equation and the second on the comparison between analytical and experimental natural frequency values, as in Cerri and Vestroni [21].

In conclusion, the possibility of identifying the damage parameters by pseudo-experimental data, both unaffected and affected by errors, is examined. The pseudo-experimental data in the applications were generated by a FEM code, and may be thought to be similar to the experimental ones, because the FEM does not keep into account all the simplifying hypotheses of the analytical model. By comparing the analytical and the numerical data, some useful remarks are made.

2. Direct problem

2.1. Undamaged arch

The continuum arch model adopted is one-dimensional. The configurations of the arch are described by the position of the points of a plane curve, the axis of the arch, and by the setting of a prototype plane region, the cross-section, continuously attached to the axis. This last can be chosen as the line joining the centroids of all the cross-sections. The sections are supposed to undergo only rigid body motions. Thus, all the fields of mechanical interest are functions of one variable only, a curvilinear abscissa along the axis in the referential configuration. The considered arch in the referential configuration has axis which is a portion of a circumference with radius R and sections orthogonal to the axis. Hence, one may introduce either an abscissa along the arch, or the corresponding angle φ spanned by the initial position radius and the considered one.

The arch kinematics is described by the tangential and radial components of the axial displacement, denoted by u and v, respectively, and the rotation of the sections, denoted by θ. Because of the one-dimensional model adopted, these fields depend only on φ and on the time,

denoted by t. Since in this paper only linear vibrations will be examined, all the fields in the following are really first order increments with respect to the referential configuration. The arch is supposed to be thin (the sections' meaningful dimension is small compared with R) and not shallow. Then, a standard assumption, verified by numerical investigations, is that the relevant behaviour of the arch is flexural [23,30,32]: the extension of the axis and the shearing strain between the cross-sections and the axis may be neglected, and the following compatibility equations are obtained:

$$v(\varphi,t)=\frac{\partial u(\varphi,t)}{\partial\varphi},\quad \theta(\varphi,t)=\frac{u(\varphi,t)}{R}+\frac{1}{R}\frac{\partial v(\varphi,t)}{\partial\varphi}=\frac{1}{R}\left(u(\varphi,t)+\frac{\partial^2 u(\varphi,t)}{\partial\varphi^2}\right). \tag{1}$$

The balance equations for the contact actions read

$$\begin{aligned}&\frac{\partial N(\varphi,t)}{\partial\varphi}-T(\varphi,t)-\mu R\frac{\partial^2 u(\varphi,t)}{\partial t^2}=0,\\ &\frac{\partial T(\varphi,t)}{\partial\varphi}+N(\varphi,t)-\mu R\frac{\partial^2 v(\varphi,t)}{\partial t^2}=0,\\ &\frac{\partial M(\varphi,t)}{\partial\varphi}-RT(\varphi,t)+JR\frac{\partial^2\theta(\varphi,t)}{\partial t^2}=0,\end{aligned} \tag{2}$$

where $N(\varphi,t)$ and $T(\varphi,t)$ are the tangential and radial components of the internal force, respectively; $M(\varphi,t)$ is the bending moment; $\mu=\rho A$ is the arch mass density per unit length, and $J=\mu I/A$ the relative mass moment of inertia per unit length, supposed ρ the mass density per unit volume, A the area of the cross-section and I the cross-sectional moment of inertia with respect to the relevant neutral axis.

Since the arch is assumed homogeneous, linearly elastic, thin, and not shallow, the constitutive equation of rectilinear beams between bending moment and increment of curvature holds and, E denoting Young's modulus by means of Eq. (1) one has

$$M(\varphi,t)=-\frac{EI}{R}\frac{\partial\theta(\varphi,t)}{\partial\varphi}=-\frac{EI}{R^2}\left(v(\varphi,t)+\frac{\partial^2 v(\varphi,t)}{\partial\varphi^2}\right). \tag{3}$$

Neglecting tangential and rotary inertia, from Eqs. (1) to (3) the simplified equation of motion is obtained

$$\frac{\partial^6 u(\varphi,t)}{\partial\varphi^6}+2\frac{\partial^4 u(\varphi,t)}{\partial\varphi^4}+\frac{\partial^2 u(\varphi,t)}{\partial\varphi^2}+\frac{\mu R^4}{EI}\frac{\partial^4 u(\varphi,t)}{\partial\varphi^2\partial t^2}=0. \tag{4}$$

Looking for natural vibration modes, the solution for Eq. (4) is assumed to have the form

$$u(\varphi,t)=U(\varphi)\exp^{\mathrm{i}\omega t}, \tag{5}$$

where $U(\varphi)$ is the natural mode, function of the spatial variable along the axis only, i is the imaginary unit, and ω is the natural circular frequency. Introducing the non-dimensional quantities

$$\chi^2=\frac{\mu R^4}{EI}\omega^2,\quad \eta=(\chi+1)^{1/2},\quad \kappa=(\chi-1)^{1/2}, \tag{6}$$

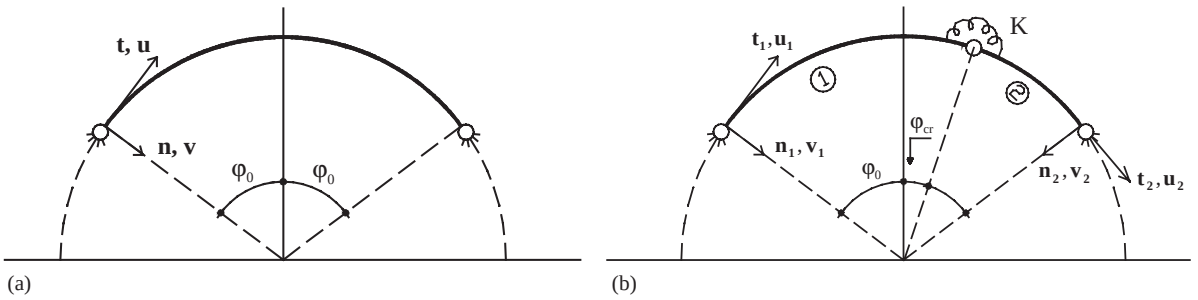

Fig. 1. Double hinged circular arch: (a) undamaged; (b) with a localised damage at φ_{cr}.

the substitution of Eqs. (5) and (6) into Eq. (4) yields the ordinary differential equation

$$\frac{\partial^6 U(\varphi)}{\partial\varphi^6} + 2\frac{\partial^4 U(\varphi)}{\partial\varphi^4} + (1-\chi^2)\frac{\partial^2 U(\varphi)}{\partial\varphi^2} = 0. \tag{7}$$

By the definitions in Eq. (6), the general solution of Eq. (7) is, A_j, $j = 1, 2, \ldots, 6$ being arbitrary real constants,

$$U(\varphi) = A_1 \sin\eta\varphi + A_2 \cos\eta\varphi + A_3 \sinh\kappa\varphi + A_4 \cosh\kappa\varphi + A_5\varphi + A_6. \tag{8}$$

An arch with opening angle $2\varphi_0$ and hinged at both ends is now considered, as shown in Fig. 1(a).

The displacement and the bending moment at both ends must vanish; hence, keeping in mind Eqs. (1), (3) and (5), the boundary conditions for Eq. (7) are $(()' = \mathrm{d}/\mathrm{d}\varphi)$

$$U(0) = U(2\varphi_0) = 0, \quad U'(0) = U'(2\varphi_0) = 0, \quad U'''(0) = U'''(2\varphi_0) = 0. \tag{9}$$

By means of Eq. (8), the expressions to be substituted into the boundary conditions (9) can be found. Thus, a homogeneous linear algebraic system in the six unknowns A_j is obtained, which admits non-trivial solutions if the determinant of the matrix of the coefficients vanishes, i.e.,

$$\det\begin{bmatrix} 0 & 1 & 0 & 1 & 0 & 1 \\ \eta & 0 & \kappa & 0 & 1 & 0 \\ -\eta^3 & 0 & \kappa^3 & 0 & 0 & 0 \\ -\eta^3\cos\eta 2\varphi_0 & \eta^3\sin\eta 2\varphi_0 & \kappa^3\cosh\kappa 2\varphi_0 & \kappa^3\sinh\kappa 2\varphi_0 & 0 & 0 \\ \eta\cos\eta 2\varphi_0 & -\eta\sin\eta 2\varphi_0 & \kappa\cosh\kappa 2\varphi_0 & \kappa\sinh\kappa 2\varphi_0 & 1 & 0 \\ \sin\eta 2\varphi_0 & \cos\eta 2\varphi_0 & \sinh\kappa 2\varphi_0 & \cosh\kappa 2\varphi_0 & 2\varphi_0 & 1 \end{bmatrix} = 0. \tag{10}$$

The explicit form of Eq. (10) is the characteristic equation of a doubly hinged undamaged circular arch:

$$\begin{aligned} &8\eta\kappa(\eta^2+\kappa^2)\sin\eta\varphi_0 \sinh\kappa\varphi_0(\varphi_0\eta\kappa(\eta^2+\kappa^2)\cos\eta\varphi_0\cosh\kappa\varphi_0 \\ &\quad - \kappa^3\cosh\kappa\varphi_0\sin\eta\varphi_0 - \eta^3\cos\eta\varphi_0\sinh\kappa\varphi_0) = 0. \end{aligned} \tag{11}$$

Table 1
Eigenvalues χ_r for the first three modes for different values of φ_0

Mode	$\varphi_0 = \pi/18$	$\varphi_0 = \pi/12$	$\varphi_0 = \pi/9$	$\varphi_0 = \pi/6$	$\varphi_0 = \pi/4$	$\varphi_0 = \pi/3$
First	323.0	143.0	80.00	35.00	15.00	8.00
Second	690.9	306.5	172.0	75.91	33.21	18.26
Third	1295	575.0	323.0	143.0	63.00	35.00
Fourth	1989	883.4	496.5	220.1	97.28	54.29

Indeed, by the definitions in Eq. (6), Eq. (11) actually contains χ, the arch non-dimensional frequency parameter, as the only unknown. Some values for χ have been obtained by solving Eq. (11) and are listed in Table 1; the results coincide with those in Henrych [23].

By means of Table 1 and of the opening angle of the arch, $2\varphi_0$, it is possible to find the rth natural circular frequency $\omega_r = \chi_r\sqrt{EI}/R^2\sqrt{\mu}$ (rad/s) and the rth natural frequency $f_r = \omega_r/2\pi$ (Hz).

2.2. Damaged arch

A damaged arch is now considered, in which the damage is localised at a section labelled by the angle φ_{cr}, counted positively clockwise with respect to the symmetry axis of the arch. The damage is represented by means of a torsion spring with stiffness K, as shown in Fig. 1(b). The value of K may be approximated supposing that the actual damage is distributed in a narrow zone of amplitude $\Delta\varphi_{cr}$, and that the average bending stiffness decrease in that zone is ΔEI. In analogy with the case of a rectilinear beam [21] it is possible to write, provided $\gamma = \Delta EI/EI$ and $\Delta\varphi_{cr}$ in radians,

$$K = \frac{(1-\gamma)}{\gamma}\frac{EI}{\Delta\varphi_{cr}R}\,. \tag{12}$$

The damaged arch then consists of two regular undamaged arches, labelled by the indexes 1 and 2 in Fig. 1(b); for each of them all the preceding results hold. In particular, the natural vibration modes of the two regular parts of the structure will be expressed by Eq. (8)

$$U_j(\varphi) = A_{j1}\sin\eta\varphi + A_{j2}\cos\eta\varphi + A_{j3}\sinh\kappa\varphi + A_{j4}\cosh\kappa\varphi + A_{j5}\varphi + A_{j6} \tag{13}$$

where A_{jk} $(j = 1,2;\ k = 1,2,\ldots,6)$ are 12 real constants of integration. In addition to the vanishing displacement of the axis and bending moment at the external hinges, the compatibility and balance equations at the inner hinge must hold. The boundary conditions at the external hinges are (Fig. 1(b))

$$U_1(0) = U_1'(0) = U_1'''(0) = 0, \quad U_2(0) = U_2'(0) = U_2'''(0) = 0. \tag{14}$$

By introducing the non-dimensional quantities

$$\psi = \frac{\varphi_{cr}}{\varphi_0}, \quad \alpha = \psi + 1, \quad \beta = \psi - 1, \quad k = \frac{K}{(EI/R)}, \tag{15}$$

the compatibility and balance equations at the inner hinge are

$$U_1(\alpha\varphi_0) - U_2(\beta\varphi_0) = 0, \quad U_1'(\alpha\varphi_0) - U_2'(\beta\varphi_0) = 0,$$
$$U_1'''(\alpha\varphi_0) - U_2'''(\beta\varphi_0) = 0, \quad U_1''(\alpha\varphi_0) + U_1^{IV}(\alpha\varphi_0) - U_2''(\beta\varphi_0) - U_2^{IV}(\beta\varphi_0) = 0,$$
$$U_1^{V}(\alpha\varphi_0) - U_2^{V}(\beta\varphi_0) = 0, \quad U_2'(\beta\varphi_0) + U_2'''(\beta\varphi_0) + k[U_2''(\beta\varphi_0) - U_1''(\alpha\varphi_0)] = 0. \tag{16}$$

The successive derivatives of $U_j(\varphi)$ are easily obtained by Eq. (13) and, substituted into the boundary conditions (16), provide a homogeneous linear algebraic system in the 12 unknowns A_{jk}, which admits non-trivial solutions if the determinant of the matrix [**C**] of the coefficients, shown in the appendix, vanishes:

$$\det[\mathbf{C}] = 0 \quad \Rightarrow \quad kg_1(\chi) + g_2(\chi, \psi) = 0. \tag{17}$$

In Eq. $(17)_2$ the expression is given of the characteristic equation of a doubly hinged damaged circular arch, where $g_1(\chi) = \det[\mathbf{A}]$, $g_2(\chi, \psi) = \det[\mathbf{B}]$, and the matrices [**A**] and [**B**], which constitute a partition of [**C**], are shown in the appendix. It is worth remarking that an equivalent expression is found when dealing with damaged beams [21], and that $g_1(\chi)$ is a function of χ alone, thus it must represent the characteristic equation of an undamaged arch. Indeed, by dividing

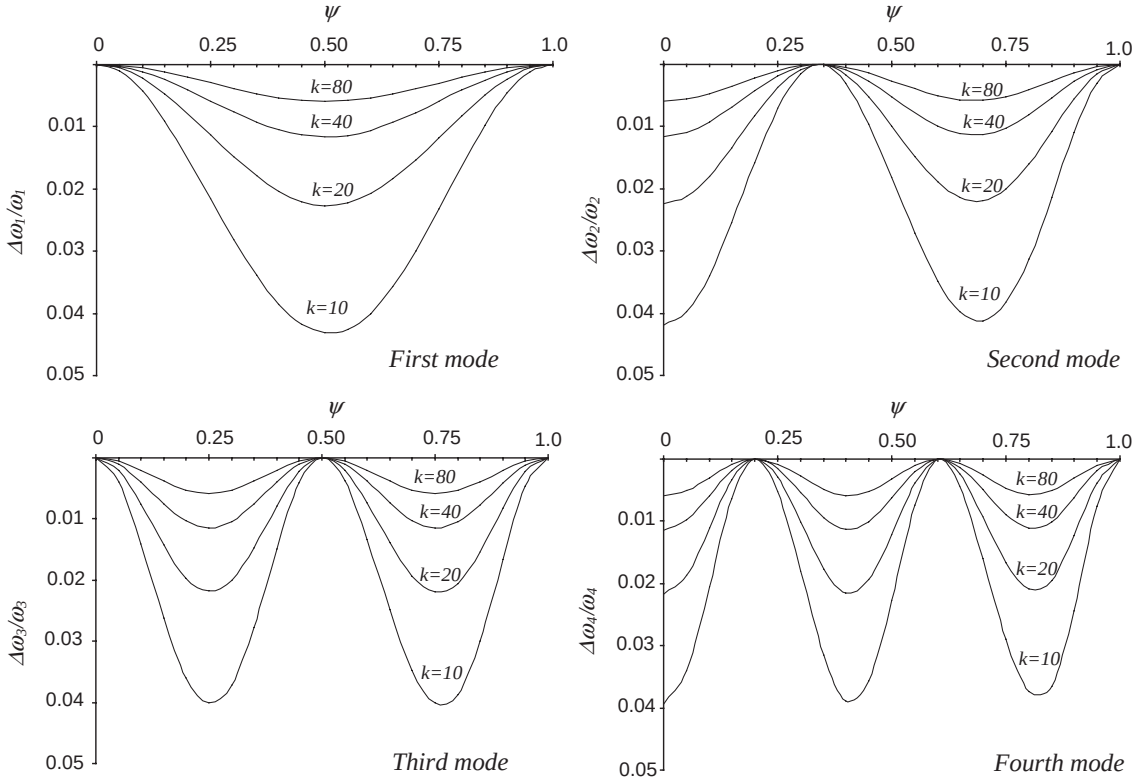

Fig. 2. Eigenfrequencies variation ratios as a function of the damage parameters ψ and k.

Eq. $(17)_2$ by k and letting k to infinity, i.e., recovering the arch integrity, the same expressions (10), (11) of the undamaged arch are obtained. It is obvious that only det[**B**] will depend on the location ψ of the damage. If k goes to zero in Eq. $(17)_2$, the characteristic equations of two doubly hinged arches will be obtained. The additive decomposition $(17)_2$ will be crucial in the development of one of the damage detection procedures. This will be shown in the next sections, where the superscripts U and D will indicate quantities as evaluated in the undamaged and damaged arch, respectively.

To show how the parameters ψ and k influence the natural frequencies of a damaged doubly hinged circular arch, an arch with opening angle $2\varphi_0 = 2(\pi/3)$ is considered. For this arch, for each mode the relative natural angular frequency variation, easily defined because of positions (6) as $\Delta\omega_i/\omega_i^U = (\omega_i^D - \omega_i^U)/\omega_i^U = (1 - \chi_i^D/\chi_i^U)$, is calculated as a function of the damage parameters.

Fig. 2 shows the curves $\Delta\omega_i/\omega_i^U$ for the first four modes of vibration. As would be expected, the natural angular frequencies decrease with the degree of damage k and depend on the position of the localised damage along the axis of the arch. Furthermore, $\Delta\omega_i/\omega_i^U$ decreases with increasing k, attains a maximum when the damage is located at a peak value of the bending curvature, while goes to zero when the damage is located at a node of the bending curvature. Remark that, because

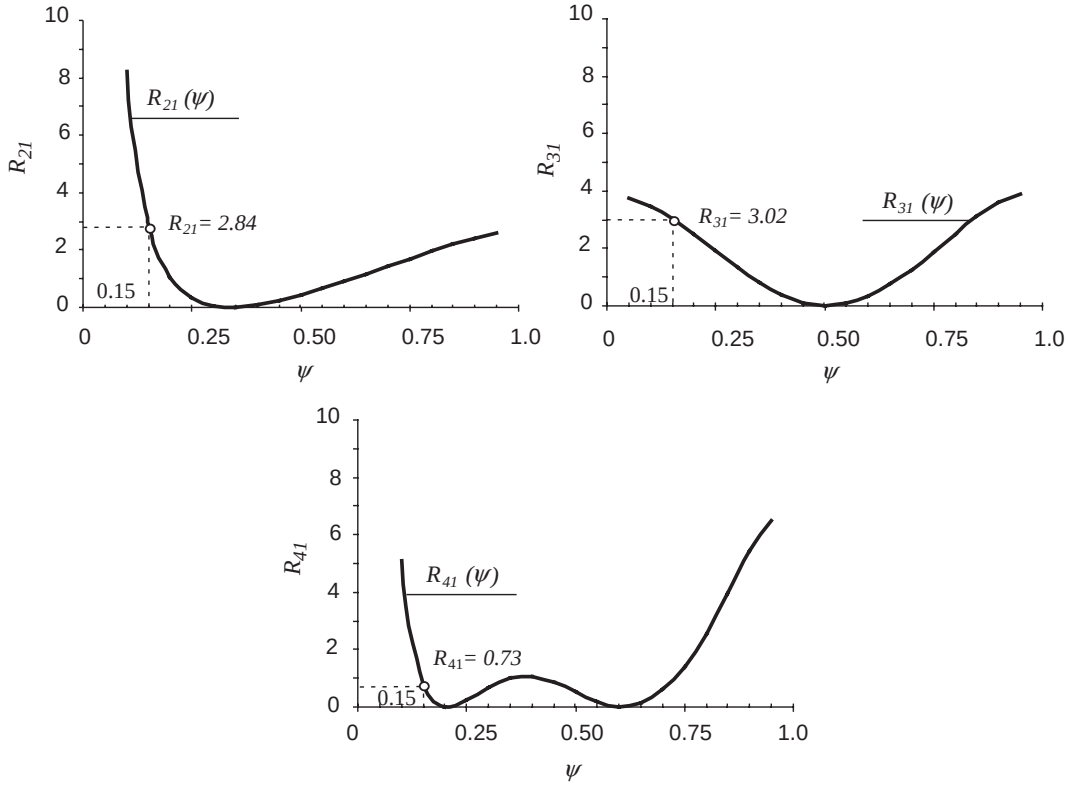

Fig. 3. R_{ij} curves versus damage parameter ψ.

of the geometry assumed in Fig. 1(b) and of position (15), the graphs actually describe what happens in the arch half to the right of the axis of symmetry.

The ratios $R_{ij} = (\Delta\omega_i/\omega_i)/(\Delta\omega_j/\omega_j)$ between the relative natural angular frequencies variations may also be considered; it turns out that R_{ij} does not depend on the damage parameter k, but only on ψ, the location of the damage, as for rectilinear beams [21]. Thus, one could use the R_{ij} as measured quantities for the damage detection procedures. Fig. 3 shows some R_{ij}-curves as a function of ψ.

3. Inverse problem

It has been shown that it is always possible, given ψ and k, to find the natural frequencies for the damaged arch, i.e., the frequency response direct problem for damaged arches is always well posed once the damage parameters are provided. More complicated is the inverse problem, which tries to detect the damage parameters once a few experimental data on the frequency response are at ease. The procedures to detect the damage parameters in general consist of two steps: first, the model must be provided for the undamaged condition, then the same must be made for the damaged condition. A comparison between the results obtained from the two models makes it possible to evaluate the damage parameters. In the following, attention is focused on the second step, as the characteristics of the undamaged arch are known.

Two procedures are introduced, as it has been done in Refs. [18–20]. The first makes direct use of the characteristic, or modal, equation of the damaged arch, while the second looks for the solution of the inverse problem as a minimum for a suitable objective function. This last, as it might be intuitively said, is based on the differences between the experimental data and those obtained by the model of the damaged arch.

3.1. The modal equation procedure

In the following, the subscript e will indicate an experimental value. It is clear from Eq. $(17)_2$ that in an arch with a localized damage, for each experimental eigenvalue $\chi^D_{e,r} = \chi^U_r(\omega^D_{e,r}/\omega^U_{e,r})$ obtained by the angular frequencies in the undamaged ($\omega^U_{e,r}$) and damaged ($\omega^D_{e,r}$) condition, it is possible to define

$$k_r(\psi) = -\frac{g_2(\chi_{e,r})}{g_1(\psi, \chi_{e,r})}. \tag{18}$$

This function of ψ only represents, for each damage location ψ, the damage intensity parameter k_r corresponding to the rth eigenvalue of the damaged arch. It is then possible to plot the curve $k_r(\psi)$ for each r; the intersection of two such curves, obtained for distinct values of r, will make it possible to evaluate k and ψ. Since the inverse problem is non-linear, however, two distinct eigenvalues could not be enough to uniquely determinate the damage parameters.

In Fig. 4 the $k_r(\psi)$-curves are shown, corresponding to the first four modes, considering a damage localised at the positions $\psi = 0.0375$, 0.1625, 0.3875, 0.6625, respectively, and of magnitude $k = 10$. Remark that not all the couples of curves $k_r(\psi)$ provide a unique intersection: for the damages D2, D3 and D4, the curves k_1 and k_2 intersect with each other twice, thus putting

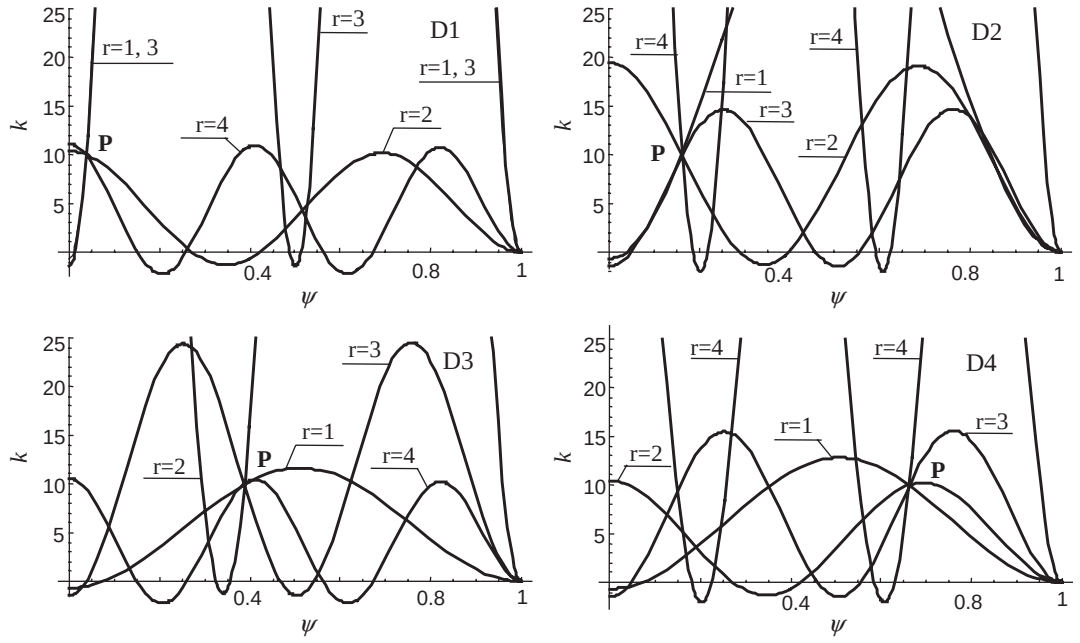

Fig. 4. Curves k_r for the first four modes without errors. P: intersection point.

into evidence two possible solutions of the inverse problem. Nevertheless, it is sufficient to add another curve to eliminate this non-uniqueness. Remember that, because of the geometry introduced in Fig. 1(b), the damage is determined modulo a reflection with respect to the axis of symmetry.

In presence of experimental and/or model errors, the measured $k_r(\psi)$-curves do not intersect at the same point, but describe a neighbourhood of the solution. It is then possible to define the function

$$m(\psi) = \sum_{r \neq s} |k_r(\psi) - k_s(\psi)|, \tag{19}$$

measuring the distance among the curves $k_r(\psi)$. To find the solution $(\bar{\psi}, \bar{k})$ of the inverse problem, the position $\bar{\psi}$ corresponding to the minimum of $m(\psi)$ is evaluated first. Then, the mean value $\bar{k}$ corresponding to $\bar{\psi}, n$ being the number of the considered k_r-curves, is determined as follows:

$$\bar{k} = \frac{\sum_r k_r(\bar{\psi})}{n}. \tag{20}$$

Fig. 5 shows the results of this approach using the first two natural frequencies without errors; for sake of convenience, the plotted function is actually $\ln(m(\psi))$. Clearly one of the identified values exactly corresponds to the expected one, while in general to obtain a unique minimum it is necessary to use at least one more natural frequency, as discussed above. All the $\ln(m(\psi))$-curves go to $-\infty$ as $\psi \to 1$; the minimum at $\psi = 1$ must be discarded because in that case the damage is located at a node of all modes, thus making the difference among the curves vanish.

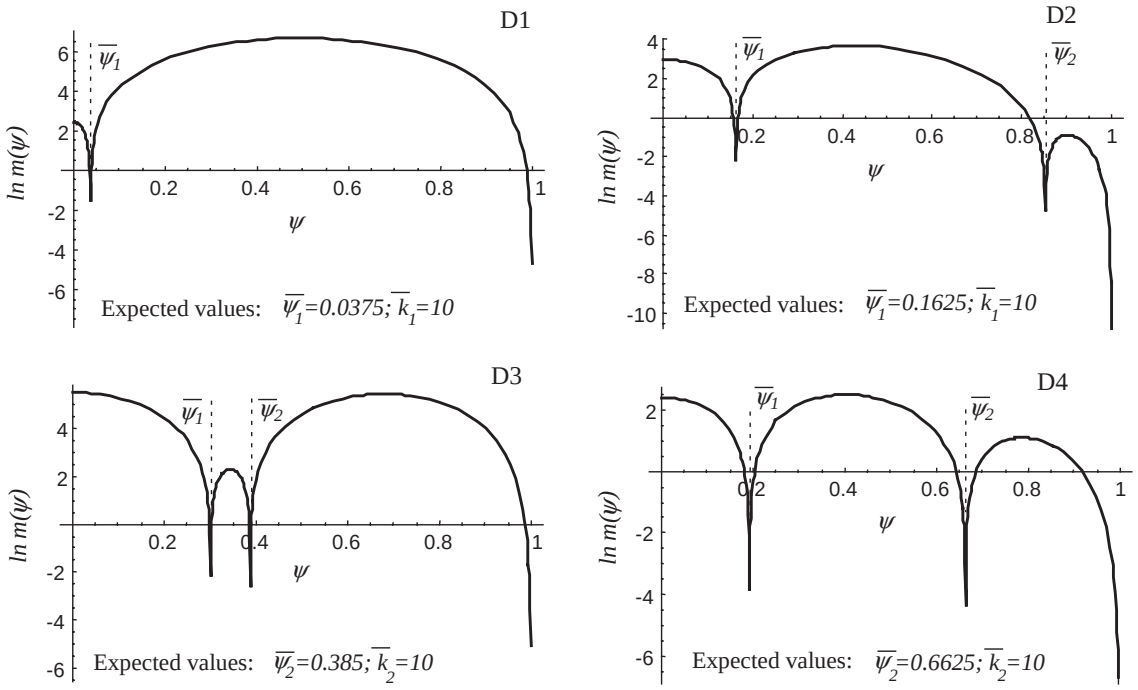

Fig. 5. $\ln m(\psi)$ curves using the first two frequencies without errors.

3.2. The response comparison procedure

The second identification procedure is based on the response comparison. An optimal estimate of the damage parameters is provided by minimising an objective function, defined via the differences between the analytical and experimental values of the variation of frequencies passing from an undamaged to a damaged state, denoted by $\Delta\omega_r(\psi,k)$ and $\Delta\omega_{e,r}$, respectively

$$l(\psi,k)=\sum_r\left|\frac{\Delta\omega_{e,r}}{\omega_{e,r}^U}-\frac{\Delta\omega_r(\psi,k)}{\omega_r^U}\right|^2, \tag{21}$$

where $\omega_{e,r}^U$ and ω_r^U are the experimental and analytical undamaged angular frequencies. The identification of the damage parameters $(\bar{\psi},\bar{k})$ is given by the minimum of the objective function (21), which may be done by successively looking for two distinct minima. First, for each damage position ψ, the minimisation of Eq. (21) with respect to k determines the function

$$\tilde{l}(\psi)=\min_k\, l(\psi,k); \tag{22}$$

the solution of the inverse problem is then given by the minimum of $\tilde{l}(\psi)$ with respect to ψ. An alternative is to use the theoretical and experimental R_{ij} as comparison parameters to locate the damage. Due to the non-linearity of the inverse problem, in general more than one curve to locate the damage is needed, as shown in Fig. 6, using the data provided in the following section.

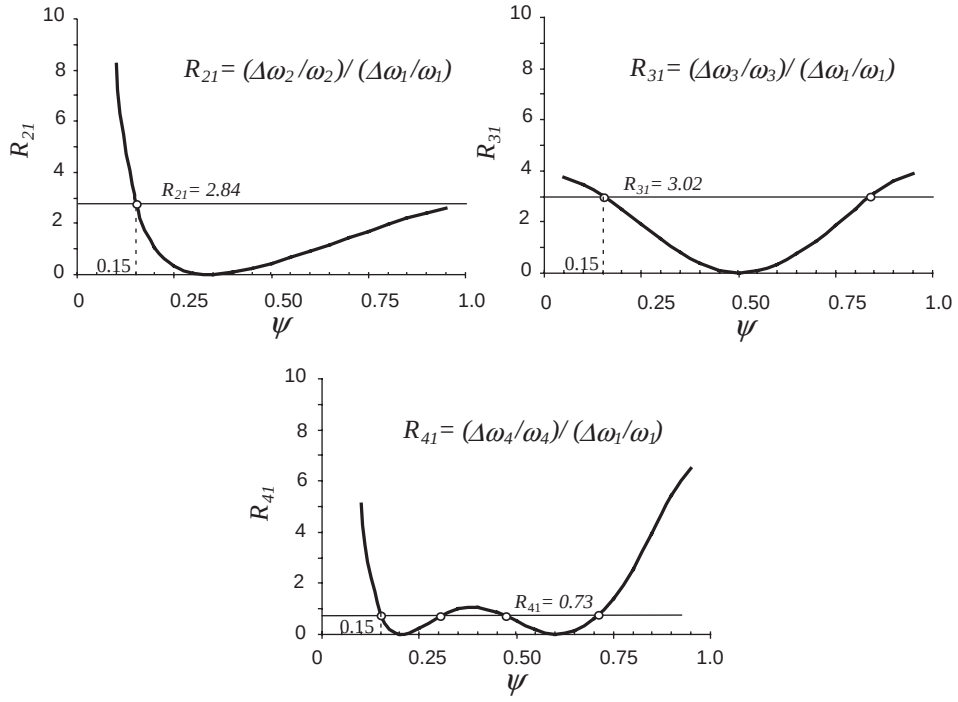

Fig. 6. Ratios R_{ij} between the eigenfrequencies variations as a function of the damage parameter ψ.

4. Examples

To test the validity of the proposed procedures, damage identification has been carried out, based on the data obtained by the FEM code STRAUS7. The considered arch is characterised by $R = 1000$ mm, $\varphi_0 = \pi/3$, $E = 2.0 \times 10^5$ N/mm^2, $\rho = 7.87 \times 10^{-9}$ T/mm^3, and has uniform rectangular cross-sections of base $B = 40$ mm and height $H = 20$ mm. The arch was divided into 80 beam elements and the search for natural parameters was performed; hence, both the first four natural frequencies and the corresponding vibration modes were found, and they are shown in Fig. 7.

As expected, the odd modes are skew-symmetric and the even modes are symmetric with respect to the axis of symmetry of the arch. Remark that a difference is present with respect to the natural frequencies obtained by means of the analytical model, due to the neglected terms in the simplified Eq. (4). Indeed, the analytical model does not take into account the extension of the axis, the shear strain, the rotary inertia actions and, most of all, the inertial tangential forces. In both the proposed methods, however, the observed quantities are not the frequencies themselves but their relative variations, so that this discrepancy does not corrupt the efficiency of the technique.

The damage was introduced by reducing the flexural rigidity of three arch elements by 50%, i.e., $\Delta EI = 50\%$. This damage is localised, since the opening angle of the damaged zone is $\Delta\varphi_{cr} = \pi/40$, and may be thus analysed using the model of torsion spring adopted here. By means of Eqs. (12) and (15), it is possible to estimate the value of the parameter k, which has been chosen to

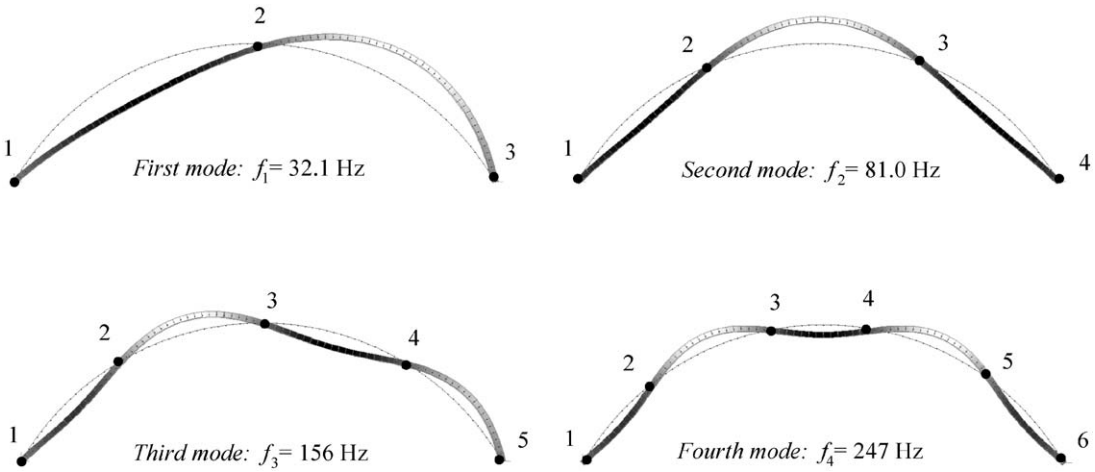

Fig. 7. Finite element model: first four circular arch mode shapes and frequencies.

Table 2
Eigenfrequencies for the undamaged and damaged arch (Hz)

Mode	Undamaged	Damage 1 $\psi = 0.0375,\ k = 13$	Damage 2 $\psi = 0.1625,\ k = 13$	Damage 3 $\psi = 0.3875,\ k = 13$	Damage 4 $\psi = 0.6625, k = 13$
First	32.09	32.07	31.83	31.15	31.19
Second	81.00	78.39	79.51	80.85	78.36
Third	156.4	156.1	152.8	154.0	153.1
Fourth	247.2	240.0	246.2	239.8	245.7

be the same for all the considered cases and equal to 13. The axis of the damage with respect to the axis of symmetry of the arch, identified in the model by the non-dimensional abscissa φ_{cr}, has been localised in four different positions: damage 1, $\varphi_{cr} = 3\pi/240$, damage 2, $\varphi_{cr} = 13\pi/240$, damage 3, $\varphi_{cr} = 31\pi/240$, damage 4, $\varphi_{cr} = 53\pi/240$; for each of the four different damaged arches the first four eigenfrequencies have been found. The results are summarised in Table 2.

To start with, the modal equation procedure will be applied, so that the k_r-curves will be plotted as a function of the position of the damage. Fig. 8 shows the results obtained for each damage position by superposing the curves relative to the first four vibration modes. It is apparent from the figures that the curves cross with each other in the vicinity of a point, which is the actual solution of the problem. As the damage introduced in the FEM calculation has been the same in all cases, the corresponding value of k was expected to be the same; and, actually, this is verified in our case. Fig. 9, in particular, shows for the considered damages the application of the approach introduced by Eqs. (19) and (20), disregarding the minimum at $\psi = 1$ of $\ln(m(\psi))$ because of the reasons reported above. Also remark that, even though there is in general no unique minimum in the plots shown in Fig. 9, there always exists an absolute minimum, which tells us the position of the localised damage. It is interesting that the expected results are recovered with only the first two

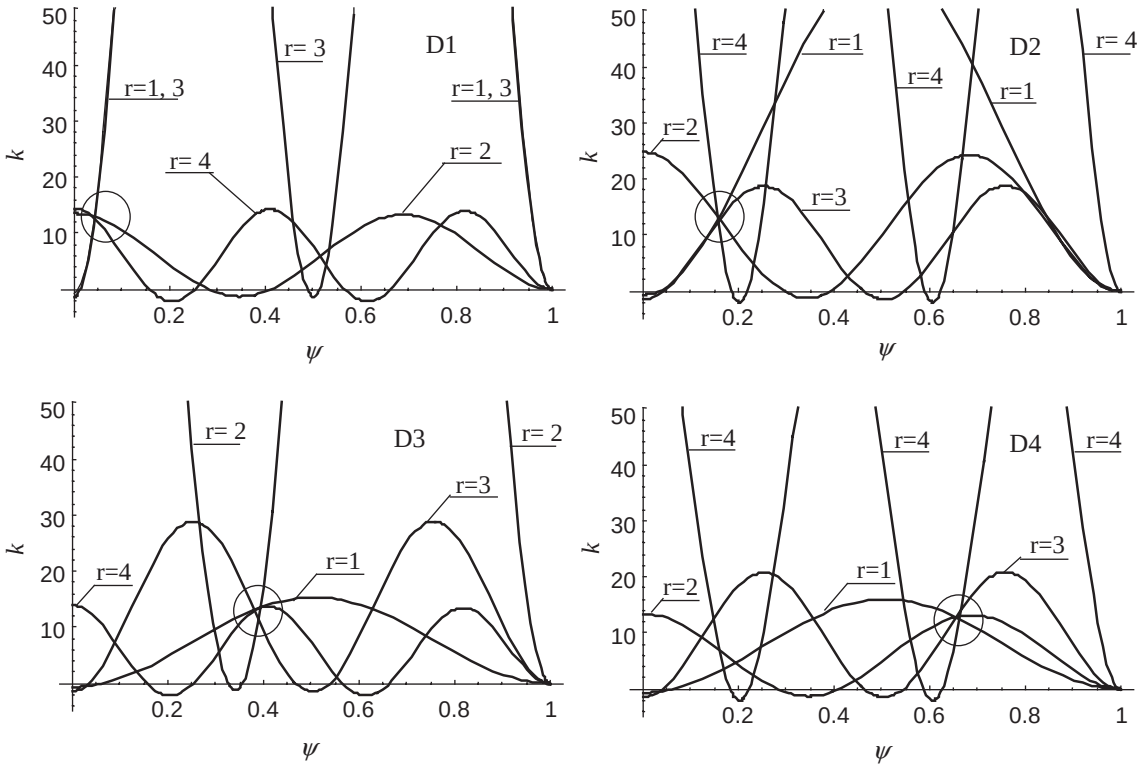

Fig. 8. Curves k_r for the first four modes.

natural frequencies; there is of course the possibility to use more frequencies, but that would not affect the validity of the procedure. The only effect of using more frequencies, indeed, would be of eliminating some of the relative minima, which can be seen in the plots of Fig. 9, and thus put into better evidence the absolute minimum which is sought.

The response comparison procedure requires the construction of the objective function $\tilde{I}(\psi)$ and the determination of its absolute minimum, see Eqs. (21) and (22). By using the same pseudo-experimental data obtained by the FEM code, the results of this technique are shown in Fig. 10, where, for each damage, two different curves are plotted versus the damage location ψ. The two curves actually represent $\log(\tilde{I}(\psi))$ and take into account the contribution of the first three and four natural frequencies, respectively. It is evident that the plotted results are satisfactory enough: indeed, this identification procedure provides numerical results for both damage parameters that are correct almost up to the second meaningful digit. A comment similar to the one made for the modal equation procedure can be made: there are relative minima, but an absolute minimum, which in absence of errors should be $-\infty$, is always easily recognisable with a very good resolution factor. In any case, a very limited number of natural frequencies is required for the proposed technique to hold; in this case, no more than three or four.

Both the proposed procedure provide a very well defined absolute minimum; the response comparison procedure, however, is more general than the modal equation procedure and may

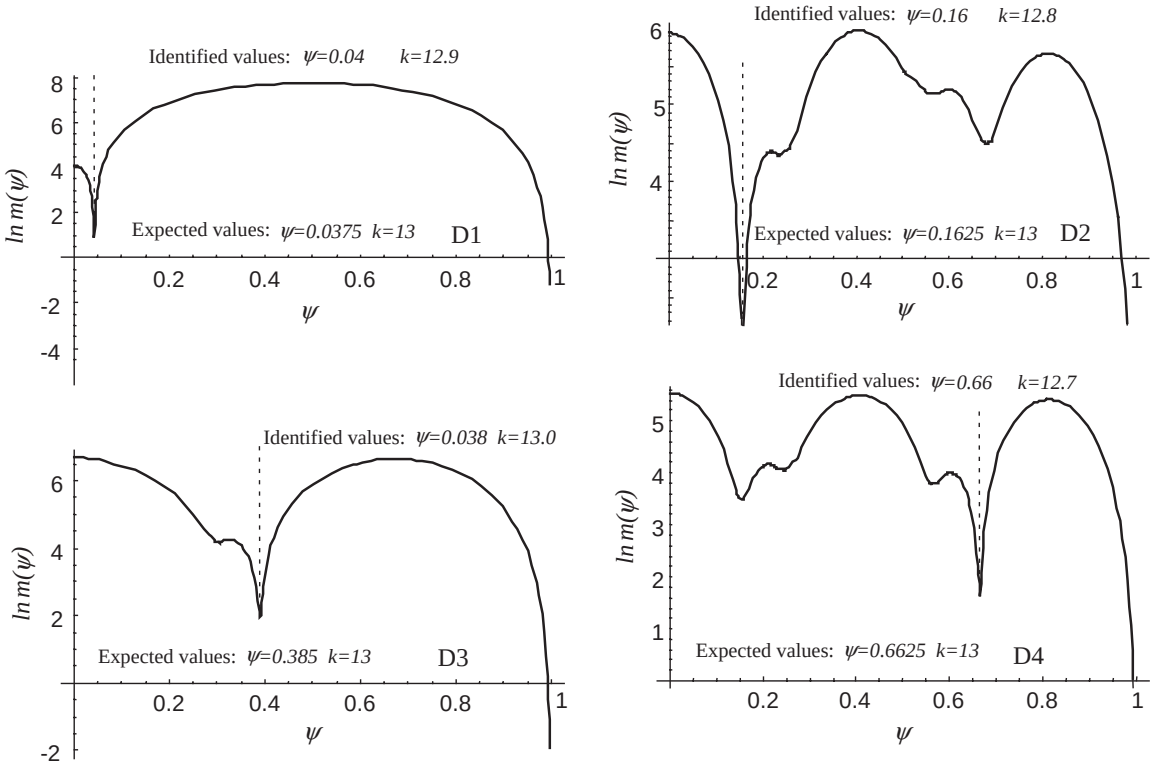

Fig. 9. $\ln m(\psi)$ curves using the first four frequencies.

easily be extended to the case in which one wants to evaluate other response characteristics, like, for example, the modal shapes or the bending stiffness.

5. Conclusions

In this paper, two different procedures to identify the damage parameters—location and magnitude of the damage—in a plane circular arch by means of measured natural frequencies are introduced. The considered arch model is one-dimensional, with relevant flexural behaviour, non-extensible centre line, vanishing shearing strain and standard linear elastic constitutive relation between bending moment and change in curvature of the axis. The damage is considered to affect a narrow zone of the arch, so to be modelled by a lumped characteristic: a torsion spring joining two adjacent sections. The procedures are based: (a) on the crossing points of some curves representing the amount of the damage, obtained by the modal equation; (b) on the minimisation of an objective function obtained by a response comparison. To show an application of the proposed procedures, pseudo-experimental data has been generated via a standard FEM code. The identification of the damage parameters is satisfactory in both techniques, and provides very

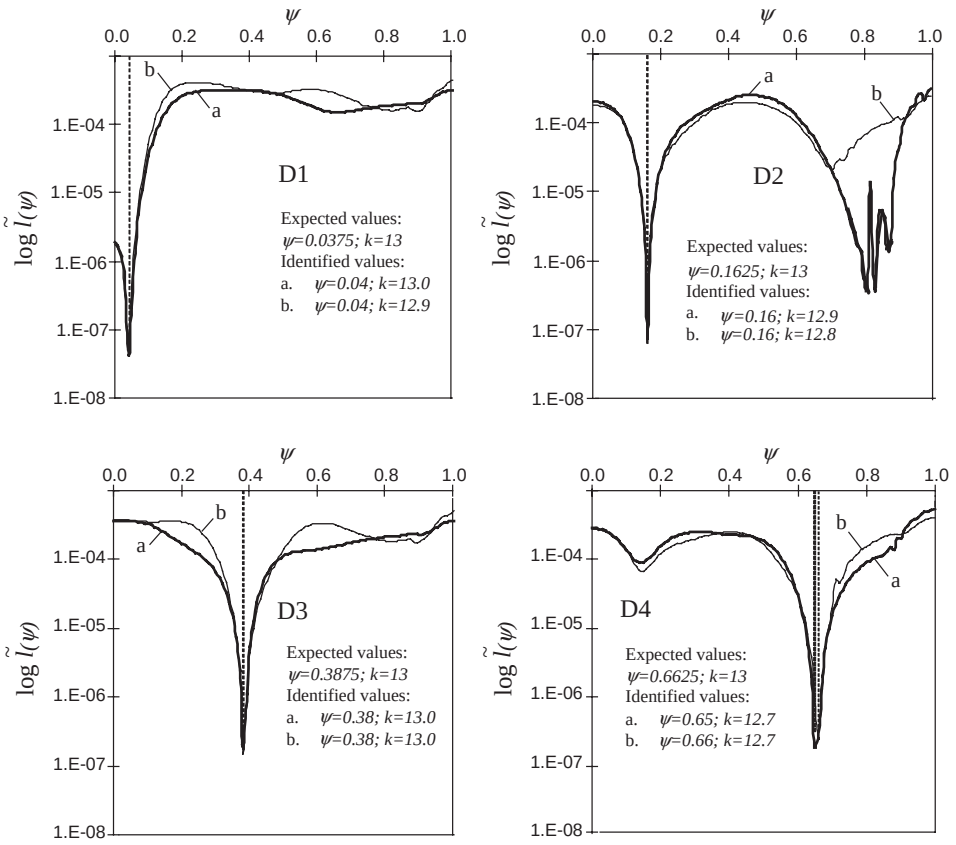

Fig. 10. Objective function $\log \tilde{l}(\psi)$ using: (a) three frequencies; (b) four frequencies.

good approximate results. Only a very limited number of natural frequencies is required; the problems do not seem to be ill-conditioned. It is easily seen that with one or two more frequencies than the first, one is provided with a satisfactory estimate of the damage parameters. While the continuum model, and, consequently, the modal equation procedure are very useful from a theoretical point of view, in practice the majority of the interpretative models are based on finite elements. In this case, the response comparison procedure results in a more natural application and may easily be extended to more complex structures.

Acknowledgements

The research is partially supported by funds of MURST from the University of Rome "La Sapienza". Giuseppe C. Ruta gratefully acknowledges the support of the "Progetto giovani ricercatori" grant of the University of Rome "La Sapienza" for the year 2000.

Appendix

Matrix [**A**]

$$\mathbf{A} = \begin{vmatrix}
0 & 1 & 0 & 1 & 0 & 1 \\
\eta & 0 & \kappa & 0 & 1 & 0 \\
-\eta^3 & 0 & \kappa^3 & 0 & 0 & 0 \\
\sin\eta\varphi_0\alpha & \cos\eta\varphi_0\alpha & \sinh\kappa\varphi_0\alpha & \cosh\kappa\varphi_0\alpha & \varphi_0\alpha & 1 \\
\eta\cos\eta\varphi_0\alpha & -\eta\sin\eta\varphi_0\alpha & \kappa\cosh\kappa\varphi_0\alpha & \kappa\sinh\kappa\varphi_0\alpha & 1 & 0 \\
-\eta^3\cos\eta\varphi_0\alpha & \eta^3\sin\eta\varphi_0\alpha & \kappa^3\cosh\kappa\varphi_0\alpha & \kappa^3\sinh\kappa\varphi_0\alpha & 0 & 0 \\
(\eta^4-\eta^2)\sin\eta\varphi_0\alpha & (\eta^4-\eta^2)\cos\eta\varphi_0\alpha & (\kappa^4+\kappa^2)\sinh\kappa\varphi_0\alpha & (\kappa^4+\kappa^2)\cosh\kappa\varphi_0\alpha & 0 & 0 \\
\eta^5\cos\eta\varphi_0\alpha & -\eta^5\sin\eta\varphi_0\alpha & \kappa^5\cosh\kappa\varphi_0\alpha & \kappa^5\sinh\kappa\varphi_0\alpha & 0 & 0 \\
-\eta^2\sin\eta\varphi_0\alpha & -\eta^2\cos\eta\varphi_0\alpha & \kappa^2\sinh\kappa\varphi_0\alpha & \kappa^2\cosh\kappa\varphi_0\alpha & 0 & 0 \\
0 & 0 & 0 & 0 & 0 & 0 \\
0 & 0 & 0 & 0 & 0 & 0 \\
0 & 0 & 0 & 0 & 0 & 0
\end{vmatrix}$$

$$\begin{vmatrix}
0 & 0 & 0 & 0 & 0 & 0 \\
0 & 0 & 0 & 0 & 0 & 0 \\
0 & 0 & 0 & 0 & 0 & 0 \\
-\sin\eta\varphi_0\beta & -\cos\eta\varphi_0\beta & -\sinh\kappa\varphi_0\beta & -\cosh\kappa\varphi_0\beta & -\varphi_0\beta & -1 \\
-\eta\cos\eta\varphi_0\beta & \eta\sin\eta\varphi_0\beta & -\kappa\cosh\kappa\varphi_0\beta & -\kappa\sinh\kappa\varphi_0\beta & -1 & 0 \\
\eta^3\cos\eta\varphi_0\beta & -\eta^3\sin\eta\varphi_0\beta & -\kappa^3\cosh\kappa\varphi_0\beta & -\kappa^3\sinh\kappa\varphi_0\beta & 0 & 0 \\
-(\eta^4-\eta^2)\sin\eta\varphi_0\beta & -(\eta^4-\eta^2)\cos\eta\varphi_0\beta & -(\kappa^4+\kappa^2)\sinh\kappa\varphi_0\beta & -(\kappa^4+\kappa^2)\cosh\kappa\varphi_0\beta & 0 & 0 \\
-\eta^5\cos\eta\varphi_0\beta & \eta^5\sin\eta\varphi_0\beta & -\kappa^5\cosh\kappa\varphi_0\beta & -\kappa^5\sinh\kappa\varphi_0\beta & 0 & 0 \\
\eta^2\sin\eta\varphi_0\beta & \eta^2\cos\eta\varphi_0\beta & -\kappa^2\sinh\kappa\varphi_0\beta & -\kappa^2\cosh\kappa\varphi_0\beta & 0 & 0 \\
0 & 1 & 0 & 1 & 0 & 1 \\
\eta & 0 & \kappa & 0 & 1 & 0 \\
-\eta^3 & 0 & \kappa^3 & 0 & 0 & 0
\end{vmatrix}$$

Matrix [**B**]

$$\mathbf{B} = \begin{vmatrix}
0 & 1 & 0 & 1 & 0 & 1 \\
\eta & 0 & \kappa & 0 & 1 & 0 \\
-\eta^3 & 0 & \kappa^3 & 0 & 0 & 0 \\
\sin \eta\varphi_0\alpha & \cos \eta\varphi_0\alpha & \sinh \kappa\varphi_0\alpha & \cosh \kappa\varphi_0\alpha & \varphi_0\alpha & 1 \\
\eta \cos \eta\varphi_0\alpha & -\eta \sin \eta\varphi_0\alpha & \kappa \cosh \kappa\varphi_0\alpha & \kappa \sinh \kappa\varphi_0\alpha & 1 & 0 \\
-\eta^3 \cos \eta\varphi_0\alpha & \eta^3 \sin \eta\varphi_0\alpha & \kappa^3 \cosh \kappa\varphi_0\alpha & \kappa^3 \sinh \kappa\varphi_0\alpha & 0 & 0 \\
(\eta^4 - \eta^2) \sin \eta\varphi_0\alpha & (\eta^4 - \eta^2) \cos \eta\varphi_0\alpha & (\kappa^4 + \kappa^2) \sinh \kappa\varphi_0\alpha & (\kappa^4 + \kappa^2) \cosh \kappa\varphi_0\alpha & 0 & 0 \\
\eta^5 \cos \eta\varphi_0\alpha & -\eta^5 \sin \eta\varphi_0\alpha & \kappa^5 \cosh \kappa\varphi_0\alpha & \kappa^5 \sinh \kappa\varphi_0\alpha & 0 & 0 \\
0 & 0 & 0 & 0 & & \\
0 & 0 & 0 & 0 & 0 & 0 \\
0 & 0 & 0 & 0 & 0 & 0 \\
0 & 0 & 0 & 0 & 0 & 0
\end{vmatrix}$$

$$\begin{vmatrix}
0 & 0 & 0 & 0 & 0 & 0 \\
0 & 0 & 0 & 0 & 0 & 0 \\
0 & 0 & 0 & 0 & 0 & 0 \\
-\sin \eta\varphi_0\beta & -\cos \eta\varphi_0\beta & -\sinh \kappa\varphi_0\beta & -\cosh \kappa\varphi_0\beta & -\varphi_0\beta & -1 \\
-\eta \cos \eta\varphi_0\beta & \eta \sin \eta\varphi_0\beta & -\kappa \cosh \kappa\varphi_0\beta & -\kappa \sinh \kappa\varphi_0\beta & -1 & 0 \\
\eta^3 \cos \eta\varphi_0\beta & -\eta^3 \sin \eta\varphi_0\beta & -\kappa^3 \cosh \kappa\varphi_0\beta & -\kappa^3 \sinh \kappa\varphi_0\beta & 0 & 0 \\
-(\eta^4 - \eta^2) \sin \eta\varphi_0\beta & -(\eta^4 - \eta^2) \cos \eta\varphi_0\beta & -(\kappa^4 + \kappa^2) \sinh \kappa\varphi_0\beta & -(\kappa^4 + \kappa^2) \cosh \kappa\varphi_0\beta & 0 & 0 \\
-\eta^5 \cos \eta\varphi_0\beta & \eta^5 \sin \eta\varphi_0\beta & -\kappa^5 \cosh \kappa\varphi_0\beta & -\kappa^5 \sinh \kappa\varphi_0\beta & 0 & 0 \\
-(\eta^3 - \eta) \cos \eta\varphi_0\beta & (\eta^3 - \eta) \sin \eta\varphi_0\beta & (\kappa^3 + \kappa) \cosh \kappa\varphi_0\beta & (\kappa^3 + \kappa) \sinh \kappa\varphi_0\beta & 1 & 0 \\
0 & 1 & 0 & 1 & 0 & 1 \\
\eta & 0 & \kappa & 0 & 1 & 0 \\
-\eta^3 & 0 & \kappa^3 & 0 & 0 & 0
\end{vmatrix}$$

Matrix [**C**]

$$\mathbf{C} = \begin{vmatrix}
0 & 1 & 0 & 1 & 0 & 1 \\
\eta & 0 & \kappa & 0 & 1 & 0 \\
-\eta^3 & 0 & \kappa^3 & 0 & 0 & 0 \\
\sin \eta\varphi_0\alpha & \cos \eta\varphi_0\alpha & \sinh \kappa\varphi_0\alpha & \cosh \kappa\varphi_0\alpha & \varphi_0\alpha & 1 \\
\eta \cos \eta\varphi_0\alpha & -\eta \sin \eta\varphi_0\alpha & \kappa \cosh \kappa\varphi_0\alpha & \kappa \sinh \kappa\varphi_0\alpha & 1 & 0 \\
-\eta^3 \cos \eta\varphi_0\alpha & \eta^3 \sin \eta\varphi_0\alpha & \kappa^3 \cosh \kappa\varphi_0\alpha & \kappa^3 \sinh \kappa\varphi_0\alpha & 0 & 0 \\
(\eta^4 - \eta^2) \sin \eta\varphi_0\alpha & (\eta^4 - \eta^2) \cos \eta\varphi_0\alpha & (\kappa^4 + \kappa^2) \sinh \kappa\varphi_0\alpha & (\kappa^4 + \kappa^2) \cosh \kappa\varphi_0\alpha & 0 & 0 \\
\eta^5 \cos \eta\varphi_0\alpha & -\eta^5 \sin \eta\varphi_0\alpha & \kappa^5 \cosh \kappa\varphi_0\alpha & \kappa^5 \sinh \kappa\varphi_0\alpha & 0 & 0 \\
-k\eta^2 \sin \eta\varphi_0\alpha & -k\eta^2 \cos \eta\varphi_0\alpha & k\kappa^2 \sinh \kappa\varphi_0\alpha & k\kappa^2 \cosh \kappa\varphi_0\alpha & 0 & 0 \\
 & & & & & \\
0 & 0 & 0 & 0 & 0 & 0 \\
0 & 0 & 0 & 0 & 0 & 0 \\
0 & 0 & 0 & 0 & 0 & 0
\end{vmatrix}$$

$$\begin{vmatrix}
0 & 0 & 0 & 0 & 0 & 0 \\
0 & 0 & 0 & 0 & 0 & 0 \\
0 & 0 & 0 & 0 & 0 & 0 \\
-\sin \eta\varphi_0\beta & -\cos \eta\varphi_0\beta & -\sinh \kappa\varphi_0\beta & -\cosh \kappa\varphi_0\beta & -\varphi_0\beta & -1 \\
-\eta \cos \eta\varphi_0\beta & \eta \sin \eta\varphi_0\beta & -\kappa \cosh \kappa\varphi_0\beta & -\kappa \sinh \kappa\varphi_0\beta & -1 & 0 \\
\eta^3 \cos \eta\varphi_0\beta & -\eta^3 \sin \eta\varphi_0\beta & -\kappa^3 \cosh \kappa\varphi_0\beta & -\kappa^3 \sinh \kappa\varphi_0\beta & 0 & 0 \\
-(\eta^4 - \eta^2) \sin \eta\varphi_0\beta & -(\eta^4 - \eta^2) \cos \eta\varphi_0\beta & -(\kappa^4 + \kappa^2) \sinh \kappa\varphi_0\beta & -(\kappa^4 + \kappa^2) \cosh \kappa\varphi_0\beta & 0 & 0 \\
-\eta^5 \cos \eta\varphi_0\beta & \eta^5 \sin \eta\varphi_0\beta & -\kappa^5 \cosh \kappa\varphi_0\beta & -\kappa^5 \sinh \kappa\varphi_0\beta & 0 & 0 \\
k\eta^2 \sin \eta\varphi_0\beta + & k\eta^2 \cos \eta\varphi_0\beta + & -k\kappa^2 \sinh \kappa\varphi_0\beta + & -k\kappa^2 \cosh \kappa\varphi_0\beta + & 1 & 0 \\
-(\eta^3 - \eta) \cos \eta\varphi_0\beta & (\eta^3 - \eta) \sin \eta\varphi_0\beta & (\kappa^3 + \kappa) \cosh \kappa\varphi_0\beta & (\kappa^3 + \kappa) \sinh \kappa\varphi_0\beta & & \\
0 & 1 & 0 & 1 & 0 & 1 \\
\eta & 0 & \kappa & 0 & 1 & 0 \\
-\eta^3 & 0 & \kappa^3 & 0 & 0 & 0
\end{vmatrix}$$

References

[1] S.W. Doebling, C.R. Farrar, M.B. Prime, A summary review of vibration-based damage identification methods, *Shock and Vibration Digest* 30 (1998) 91–105.

[2] O.S. Salawu, Detection of structural damage through changes in frequencies: a review, *Engineering Structures* 19 (1997) 718–723.

[3] P. Cawley, R.D. Adams, The location of defects in structures from measurements of natural frequencies, *Journal of Strain Analysis* 14 (1979) 49–57.

[4] T.G. Chondras, A.D. Dimarogonas, Identification of cracks in welded joints of complex structures, *Journal of Sound and Vibration* 69 (1980) 531–538.
[5] S. Christides, A.D.S. Barr, One-dimensional theory of cracked Bernoulli–Euler beams, *International Journal of Mechanical Sciences* 26 (1984) 639–648.
[6] G.M.L. Gladwell, The inverse problem for the vibrating beams, *Proceedings of the Royal Society of London, Series A* 393 (1984) 277–295.
[7] M.M. Yuen, A numerical study of the eigenparameters of a damaged cantilever, *Journal of Sound and Vibration* 103 (1985) 301–310.
[8] R.Y. Liang, F. Choy, J. Hu, Identification of cracks in beam structure using measurements of natural frequencies, *Journal of Franklin Institute* 324 (1990) 505–518.
[9] R.Y. Liang, J. Hu, F. Choy, Quantitative NDE technique for assessing damages in beam structures, *Journal of Engineering Mechanics* 118 (1992) 1469–1487.
[10] P.F. Rizos, N. Aspragathos, A.D. Dimarogonas, Identification of crack location and magnitude in a cantilever beam from the vibration modes, *Journal of Sound and Vibration* 138 (1990) 381–388.
[11] W.M. Ostachowicz, M. Krawczuk, Analysis of the effect of a crack on the natural frequencies of a cantilever beam, *Journal of Sound and Vibration* 150 (1991) 191–201.
[12] M.H.H. Shen, J.E. Taylor, An identification problem for vibrating cracked beam, *Journal of Sound and Vibration* 150 (1991) 457–484.
[13] A. Morassi, Crack-induced changes in eigenparameters of beam structures, *Journal of Engineering Mechanics* 119 (1993) 1798–1803.
[14] A. Morassi, Identification of a crack in a rod based on changes in a pair of natural frequencies, *Journal of Sound and Vibration* 242 (2001) 577–596.
[15] T.G. Chondras, A.D. Dimarogonas, J. Yao, A continuous cracked beam vibration theory, *Journal of Sound and Vibration* 215 (1998) 17–34.
[16] Y. Narkis, Identification of crack location in vibrating simply supported beams, *Journal of Sound and Vibration* 172 (1994) 549–558.
[17] M. Boltezar, B. Strancar, A. Kuhelj, Identification of transverse crack location in flexural vibrations of free-free beams, *Journal of Sound and Vibration* 211 (1998) 729–734.
[18] F. Vestroni, D. Capecchi, Damage evaluation in cracked vibrating beams using experimental frequencies and finite element models, *Journal of Vibration and Control* 2 (1996) 69–86.
[19] D. Capecchi, F. Vestroni, Monitoring of structural systems by using frequency data, *Earthquake Engineering and Structural Dynamics* 28 (1999) 447–461.
[20] F. Vestroni, D. Capecchi, Damage detection in beams structures based on frequency measurements, *Journal of Engineering Mechanics* 126 (2000) 761–768.
[21] M.N. Cerri, F. Vestroni, Detection of damage in beams subjected to diffused cracking, *Journal of Sound and Vibration* 234 (2000) 259–276.
[22] J.K. Sinha, M.I. Friswell, S. Edwards, Simplified models for the location of cracks in beam structures using measured vibration data, *Journal of Sound and Vibration* 251 (2002) 13–38.
[23] J. Henrych, *Dynamics of Arches and Frames*, Elsevier, Amsterdam, 1981.
[24] H. Lamb, On the flexure and the vibrations of a curved bar, *Proceedings of the London Mathematical Society* 19 (1888) 365–376.
[25] A.E.H. Love, *A Treatise on the Mathematical Theory of Elasticity*, Dover, New York, 1944.
[26] N.M. Auciello, M.A. De Rosa, Free vibrations of circular arches: a review, *Journal of Sound and Vibration* 176 (1994) 433–458.
[27] P. Chidamparam, A.W. Leissa, Vibrations of planar curved beams, rings and arches, *Applied Mechanics Reviews* 46 (1993) 467–483.
[28] F.W. Waltking, Schwingungszahlen und Schwingungsformen von Kreisbogentragern, *Ingenieur-Archiv* 5 (1934) 429–449.
[29] J.P. Den Hartog, The lowest natural frequency of circular arcs, *Philosophical Magazine* 7 (5) (1928) 400–408.
[30] L.L. Philipson, On the role of extension in the flexural vibrations of rings, *Journal of Applied Mechanics* 23 (1956) 364–366.

[31] S.S. Rao, V. Sundararajan, In-plane flexural vibrations of circular rings, *Journal of Applied Mechanics* E36 (1969) 620–625.
[32] A.S. Veletsos, W.J. Austin, C.A. Lopes Pereira, S.-J. Wung, Free in-plane vibrations of circular arches, *Journal of the Engineering Mechanics Division, American Society of Civil Engineers* 98 (1972) 311–329.
[33] A. Krishnan, S. Dharmaj, Y.J. Suresh, Free vibration studies of arches, *Journal of Sound and Vibration* 186 (1995) 856–863.
[34] E. Tüfekçi, A. Arpaci, Exact solutions of in-plane vibrations of circular arches with account taken of axial extension, transverse shear and rotatory inertia effects, *Journal of Sound and Vibration* 209 (1998) 845–856.
[35] X. Tong, N. Mrad, B. Tabarrok, In-plane vibration of circular arches with variable cross-sections, *Journal of Sound and Vibration* 212 (1998) 121–140.
[36] M. Krawczuk, W.M. Ostachowicz, Natural vibrations of a clamped–clamped arch with an open transverse crack, *Journal of Vibration and Acoustics* 119 (1997) 145–151.